A. Alwadie / International Journal of Engineering Research and Applications (IJERA) ISSN: 2248-9622 www.ijera.com
Vol. 2, Issue 6, November- December 2012, pp.501-512

High Performance Predictive Direct Torque Control Of Induction Motor Drives System

A. Alwadie
Electrical Engineering Department, Faculty of Engineering, Najran University, KSA

ABSTRACT

This paper presents a practical implementation for direct torque control of induction motor drive. Control system experiment is proposed using Digital Signal Processor. This control scheme directly determines the switching states of the inverter and gives optimal characteristics for stator flux and torque control. A simple switching pattern for direct torque control algorithm for induction motor drives has been presented. The main results with the simple approach are greatly reduced torque pulsations, constant and controlled switching frequency. Results show that the simulation meets the experimental results.

Keywords - Digital Signal Processor (DSP) - Induction Motor (IM) - Direct Torque Control (DTC) - Space Vector Modulation.

1. INTRODUCTION

Nowadays, field oriented control (FOC) and direct torque control (DTC) is amongst the most important control methods and is extensively used in induction motor drives. High performance induction motor drives without position sensors are desired for industrial applications. From this point, DTC is a suitable technique for squirrel-cage induction motors. In this technique, the stator flux is implemented by measuring the stator voltage and currents in a similar way that is done in direct FOC technique. On the other hand, the correct choice of the inverter voltage vector leads to direct and decoupled control of motor flux and torque. According to this novel concept of decoupling DTC is seen to be different from FOC and it has satisfied some advantages like simplicity and quick torque response [1:3].

In this paper, a control method is proposed that can provide transient performance similar to DTC with reduced torque pulsations at steady state. The inverter switching pattern is determined over constant switching period and hence constant switching frequency is obtained. The torque and flux controller design is investigated using a sliding mode controller for direct torque control. Moreover, the complete power circuits such as (Power supply, Rectifier, pulse width modulation (PWM) inverter, power interface, current sensors, voltage sensors, and DSP board) are implemented and configured. In addition, Implementation of Digital Signal Processor (DSP1102) on DTC has been presented. Through the implementation, it will be shown that the high performance of the control system is achieved. Computer simulation validates the experimental results of this control method.

2. DIRECT TORQUE CONTROL MODELING

A detailed block diagram of the direct torque controlled induction motor drive is shown in Fig.(1). The figure shows a quick response of the torque control system in which the instantaneous speed (ω_s) of the primary flux linkage vector (y_s)of the motor is controlled in such a way that it allows the developed torque (T_d) to agree with the torque command (T^*) within a certain error. y_s and T_d are calculated respectively by the following relations [4]:

$$\psi_s = \int (v_s - R_s i_s)\, dt \qquad (1)$$

$$T_d = \frac{3}{2} p\left(\psi_{ds} i_{qs} - \psi_{qs} i_{ds}\right) \qquad (2)$$

Where,
V_s the instantaneous space primary voltage vector.
i_s the instantaneous space primary current vector.
R_s the primary winding resistance.
y_{ds}, y_{qs} d-axis and q-axis stator flux.
i_{ds}, i_{qs} d-axis and q-axis stator current.

From equation (1), it is clear that y_s can be directly controlled by v_s because of small stator winding resistance drop. It is generally known that there are eight voltages made by a three-phase inverter. By proper selecting of these vectors both the amplitude and speed of y_s are controlled to regulate the instantaneous value of T_d as it will be shown later.

2.1 Control system configuration

For the purpose of control design, it is necessary to know a dynamic model of the induction motor, which incorporates all dynamic effects occurring during steady state and transient operation. The state equations of the induction motor are given by [5]:

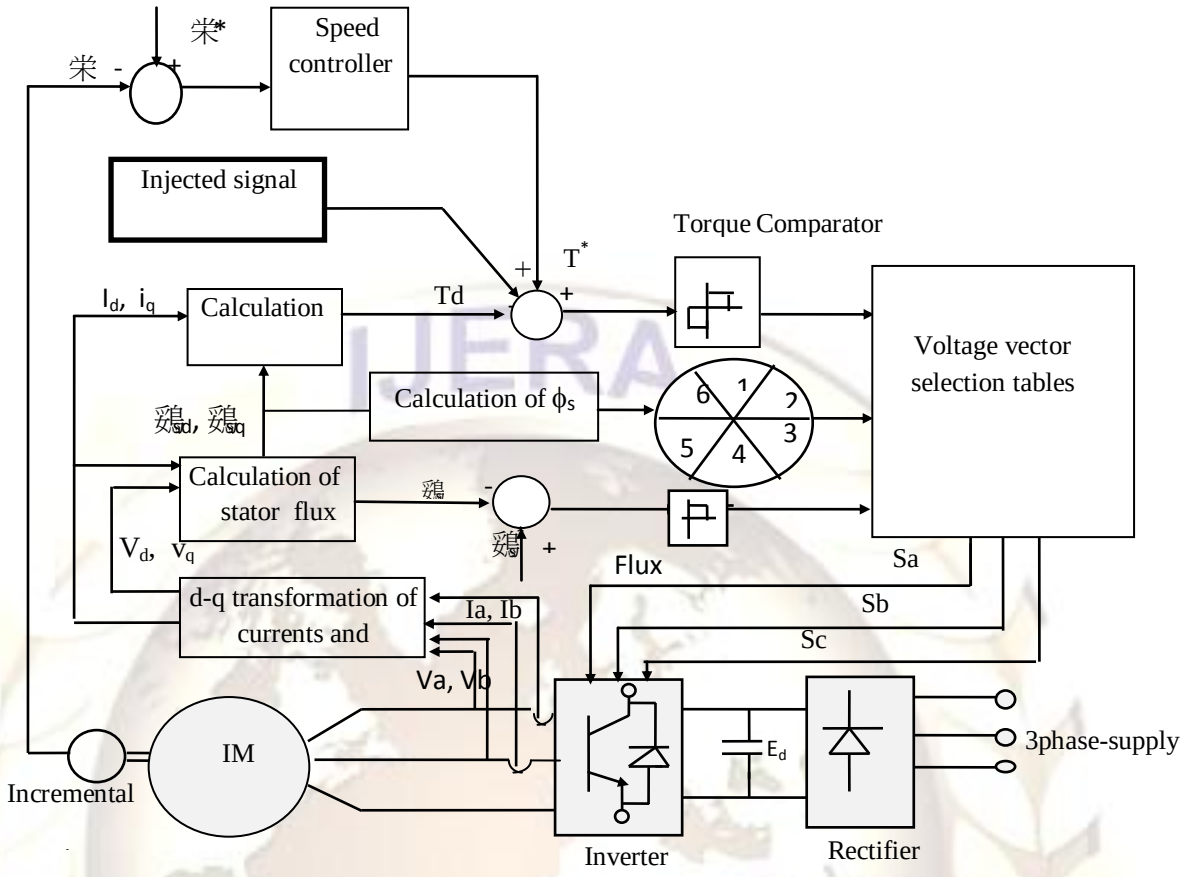

Fig.(1) Schematic diagram of direct torque control system

$$\begin{bmatrix} \frac{di_{ds}}{dt} \\ \frac{di_{qs}}{dt} \\ \frac{di_{dr}}{dt} \\ \frac{di_{qr}}{dt} \end{bmatrix} = \begin{bmatrix} \frac{1}{\sigma L_s} V_{ds} \\ \frac{1}{\sigma L_s} V_{qs} \\ -\frac{L_m}{\sigma L_s L_r} V_{ds} \\ -\frac{L_m}{\sigma L_s L_r} V_{qs} \end{bmatrix} + \begin{bmatrix} -\frac{R_s}{\sigma L_s} & \frac{L_m^2 p\omega_r}{\sigma L_s L_r} & \frac{R_s L_m}{\sigma L_s L_r} & \frac{L_m p\omega_r}{\sigma L_r} \\ -\frac{L_m^2 p\omega_r}{\sigma L_s L_r} & -\frac{R_s}{\sigma L_s} & -\frac{L_m p\omega_r}{\sigma L_r} & \frac{L_m R_s}{\sigma L_s L_r} \\ \frac{R_s L_m}{\sigma L_s L_r} & -\frac{L_m p\omega_r}{\sigma L_r} & -\frac{R_r}{\sigma L_r} & -\frac{\omega_r}{\sigma} \\ \frac{L_m p\omega_r}{\sigma L_r} & \frac{L_m R_s}{\sigma L_s L_r} & \frac{\omega_r}{\sigma} & -\frac{R_r}{\sigma L_r} \end{bmatrix} \begin{bmatrix} i_{ds} \\ i_{qs} \\ i_{dr} \\ i_{qr} \end{bmatrix} \quad (3)$$

where,

L_{ls} stator winding leakage inductance per phase.

L_{lr} rotor winding leakage inductance per phase.

L_m mutual inductance per phase referred to the stator.

S total equivalent leakage factor of the motor.

$$\left(\sigma = 1 - \frac{L_m^2}{L_s L_r}\right)$$

L_s stator winding inductance per phase($L_s = L_{ls} + L_m$).

L_r rotor winding inductance per phase($L_r = L_{lr} + L_m$).

The instantaneous space vectors of the PWM inverter are regarded as discrete values, and the analysis using the instantaneous vectors is suitable for investigating the dynamic behavior of the motor. To treat three phase quantities as a whole, the three phase machine voltages and currents are represented by an instantaneous space voltage vector (v_s) and an instantaneous space current vector (i_s), respectively, as [6]:

$$v_s = \sqrt{\frac{2}{3}} \left[v_a + v_b e^{j\frac{2\pi}{3}} + v_c e^{j\frac{4\pi}{3}} \right] \quad (4)$$

$$i_s = \sqrt{\frac{2}{3}}\left[i_a + i_b e^{j\frac{2\pi}{3}} + i_c e^{j\frac{4\pi}{3}} \right] \quad (5)$$

where, v_a, v_b and v_c are the instantaneous values of the primary line-to-neutral voltages and i_a, i_b and i_c are the instantaneous values of the primary line-to-neutral currents.

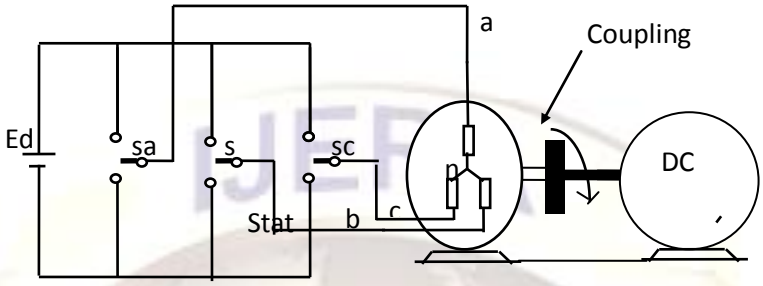

Fig.(2) Schematic diagram of PWM inverter fed induction motor drive.

Schematic diagram of the PWM fed induction motor drive is shown in Fig.(2), where S_a, S_b, and S_c are the switching functions with the value of 1 when the switch is set to positive voltage or 0 when the switch is set to negative voltage.

Considering the combinations of the status of switches, the inverter has eight conduction modes[7,8]. By using these switching functions the primary space voltage vector can be expressed as:

$$v_s(S_a, S_b, S_c) = \sqrt{\frac{2}{3}} E_d \left(S_a + S_b e^{j\frac{2\pi}{3}} + S_c e^{j\frac{4\pi}{3}} \right) \quad (6)$$

where, E_d is the dc link voltage of the inverter.

According to the combinations of switching modes, the primary space voltage vectors $v_s(S_a, S_b, S_c)$ is specified for eight kinds of vectors $v_s(1,1,1)$, (0,0,0) and the others are the space nonzero active voltage vectors. i.e.(1,0,0),……..(0,1,1), as shown in Fig.(3) and according to table(1).

Table (1)

N(switching mode)	1	2	3	4	5	6	7	8
phase-a	1	0	0	0	1	1	1	0
phase-b	1	1	1	0	0	0	1	0
phase-c	0	0	1	1	1	0	1	0

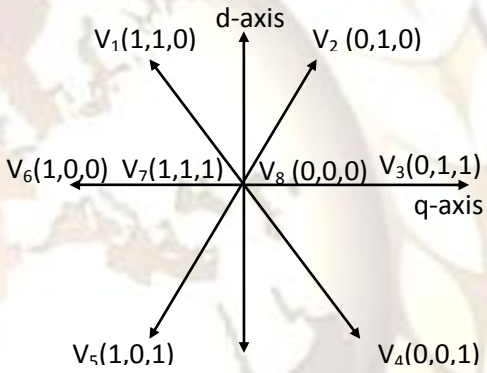

Fig.(3) Representation of primary space voltage vectors.

2.2 DTC STATE VARIABLE SELECTION

The direct torque control is achieved using three state variables [9]. The first variable is the difference between the command stator flux and the estimated stator flux magnitude, the second state variable is the difference between the command torque and the estimated electromagnetic torque, and the third one is the angle of stator flux. The control variables of the direct torque control can be investigated using Fig.(4-a), Fig.(4-b) as follows. Looking at the flux position in Fig (4-a) it is noticed that, states 3,4,5 will increase the flux while states 2,1,6 will decrease it. Similarly, states 4, 3, 2 will increase the current (i.e. the torque) while states 1,6,5 will decrease it. Gathering these states, it is found that for a large increase in flux and a small increase in torque, state 4 is selected, for a small increase in flux and a large increase in torque, state 3 is selected, for a small decrease in flux and a small increase in torque, state 2 is selected, for a large decrease in flux and a small decrease in torque, state 1 is selected, for a small decrease in flux and a large decrease in torque, state 6 is selected, for a small increase in flux and a large decrease in torque, state

5 is selected, and for a small decrease in torque and a constant flux, state 0 is selected.

3. SLIDING MODE DIRECT FLUX AND TORQUE CONTROLLER DESIGN

In order to achieve a high level of ac motor control, it is necessary to keep the flux as nearly as constant except for the field weakening region [3,4]. In case of sinusoidal ac power supplies the trajectory of primary flux is a smooth circle unlike, it happens in electronic inverters, which is not purely sinusoidal. Therefore, it is difficult to keep the air gap flux constant especially in the low speed region. The instantaneous space vector approach has made it possible to trace the primary flux and keep it almost constant. The primary space flux vector of induction motor can be calculated by equation (1). Assuming that the voltage drop of the primary winding resistance is small, the trajectory of y_s moves in the direction of v_s (S_a, S_b, S_c), the velocity of space non zero voltage vector gives the direction and the amplitude of y_s , but by applying a space zero voltage vector to an induction motor, the movement of y_s will be stopped. Therefore, by selecting these vectors appropriately, the trajectory of y_s will follow the specified locus. i.e. by selecting adequate voltage vectors, y_s can be kept almost constant and the rotating velocity of y_s can be controlled by changing the output ratio between zero vectors and the remaining non zero vectors. So, ω_s and y_s are greatly concerned with the direct torque control. In DTC system under study, constant flux can be obtained by comparing the primary flux with the command flux. The output of the flux comparator will be as follows:

$\varepsilon y = 1$ when $y_s < y_s^*$., and

$\varepsilon y = 0$ when $y_s > y_s^*$.

where, e denote the error signal in both y_s and T_d.

In the six step inverter, the d-q plane can be divided into six regions resulting from the general case:

$(2N-3)p/6 = <f_n <= (2N-1)p/6$ where; N=1,2,……6.

Since the flux is kept almost constant, the torque is then proportional to ω_s (instantaneous-slip angular velocity). As mentioned above, the velocity of the primary flux is proportional to the dc link voltage, and the direction of rotation of the primary flux is determined by the active voltage vectors and the movement of the primary flux will be stopped when zero voltage vectors is applied. Therefore, by changing the ratio of the number of active and zero voltage vectors, the slip angular velocity can be regulated. Hence, the direct torque control is obtained by adequate selection between active and zero voltage vectors. Hence, when the torque T_d is small compared with T^* it is necessary to increase T_d as fast as possible by applying the fastest ω_s. On the other hand, when T_d reaches T^* it is better to decrease T_d as slowly as possible. Thus the output of the torque controller can be classified as follow:

$\varepsilon T=1$ if $T_d < T^*$

$\varepsilon T=0$ if Td= T*

(8)

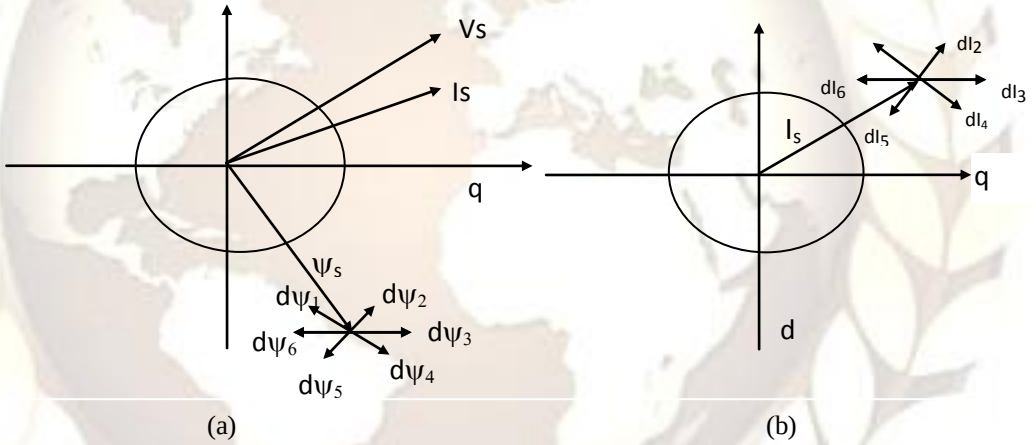

Fig.(4) Vector diagram illustrating the state selection process of flux and torque during transient operation.

$\varepsilon T=-1$ if Td>T*

The output of the torque controller is a three level hysteresis comparator. Using the three variables, εy, εT and the stator flux position $f = (\tan^{-1} y_d / y_q)$, the following optimum switching tables (2), and (3) are obtained. Accordingly, accessing the tables, in which the inverter output voltages are given by the output of the two comparators and the angle f(n), the optimum switching model (base drive signals) desirable for driving the base of the inverter can be obtained.

The inverter output voltage is then defined as in equation (6). The entire system has been verified using Matlab, Simulink and the following simulation results has been obtained.

Table (2)

ε□ □	εT	□1	□2	□3	□4	□5	□6
0	1	V_2	V_3	V_4	V_5	V_6	V_1
0	0	V_8	V_7	V_8	V_7	V_8	V_7
0	-1	V_4	V_5	V_6	V_1	V_2	V_3

Table (3)

ε□ □	εT	□1	□2	□3	□4	□5	□6
1	1	V_1	V_2	V_3	V_4	V_5	V_6
1	0	V_7	V_8	V_7	V_8	V_7	V_8
1	-1	V_5	V_6	V_1	V_2	V_3	V_4

3.1 STATOR FLUX ESTIMATION ANALYSIS

In order to have a fast acting and accurate control of induction motor, the flux linkage of the motor must be measured. However, it is difficult and expensive. Therefore, it is preferred to estimate the motor flux linkage based on measurement of motor voltages, currents and speed if it is required. There are several flux estimation techniques, some of them work with stator flux while others prefer rotor flux. As stator flux control is used in the experiment, the estimators discussed here are mainly stator flux estimators. Two cases are considered throughout this study: first, neglecting the rotor current while the motor is running at no load, the second is to consider the rotor current during load condition.

- **Stator flux estimation using dc link voltage and two line currents (voltage model)**

One desirable feature of direct torque control, or any control method based on stator flux control is to consider usually the stator flux as an estimated quantity using terminal measurements [6]. At first, simple flux estimator is obtained from equation (1) in integral form which is known as voltage model [7]. The input signals to this estimator are measured stator currents and voltages and if these signals are without errors like offset, noise and if the stator resistance is well tuned, then this estimator will be a perfect solution even if the rotor current is considered not to be zero. In fact this estimator is difficult to be used in practice, because of the acquired error signals, offset and drift in the integrating hardware. As a result, accumulation of these errors will exist if there is no feedback from the integrator output to the input. The resulting run away is a fundamental problem of pure integration. However, the challenges in stator flux estimation appear at low frequencies especially when the stator resistance drop is in the same order of the stator voltage. The problems related to drifting integrators are often pointed out as the main difficulties with flux estimation at low speeds and a solution to stator flux estimation will be presented later.

- **Stator flux estimation using motor speed and two line currents (current model)**

One way to eliminate the drift is to use the rotor model in stator coordinate equation (9) in which the required signals to be measured are stator currents and rotor speed.

$$\frac{d\psi_r}{dt} = \frac{R_r * L_m * i_s}{L_r} - \psi_r\left(\frac{R_r}{L_r} - j\omega_r\right) \quad (9)$$

$$\psi_s = i_s\left(L_s - \frac{Lm \uparrow 2}{L_r}\right) + \frac{L_m}{L_r}\psi_r \quad (10)$$

The accuracy of this estimator depends on the correct setting of the motor parameters particularly on the rotor time constant which is a critical and the mutual inductance which is less critical. This estimator has good properties at low speeds; however, it is sensitive to parameter errors at high frequency.

- **Stator flux estimation using flux observer**

As the voltage model estimator has good properties at high frequency and the current model estimator has good properties at low frequency, various ways have been tried to combine them. A straightforward way of combination is adopted [4] using a low pass filter where the current model estimator and the voltage model estimator are selected at low and high frequency, respectively. The same idea of combining the voltage and current models to obtain a flux estimator at all speeds is observed in [8]; however, instead of using a low pass filter to combine the models an observer topology is created which uses a closed loop linear controller with two deterministically set gains to govern the transition between the low and high speed estimators. However, the drawback of this type of observer is that they require a speed or position information using a shaft sensor and if the speed information can be obtained without sensor then a wide speed range flux estimation could be achieved.

The attractive feature of stator flux regulated, rotor flux oriented control technique is that it is capable of achieving correct torque and flux control even under detuned conditions [9]. It is clear that the performance of flux estimation depends on voltages, currents and the model parameter matching.

3.2 IMPROVED STATOR FLUX ESTIMATION

Induction motor stator flux estimation has taken a lot of interest as it is used with several control techniques, such as, classical DTC, stator flux field oriented control. Even though Stator flux can be measured [10], this is really difficult and expensive; consequently, the flux is preferred to be estimated based on measurement of voltages,

currents and velocity if it is required. Several problems are still under investigation like zero speed operation without speed sensor. The main reasons related to the voltage model are offset and drift component in the acquired signals and the increased sensitivity to stator resistance variation. These reasons decrease the accuracy of stator flux estimation around zero speed. Other difficulties arises if the dc link voltage and the switching signals of the inverter are used to calculate the stator flux, one is the voltage drop across the power devices themselves, the other is the voltage losses due to dead time between two inverter switches in the same branch. The exact voltage calculation is difficult with respect to the dead time, but these two errors must be compensated. A simple solution is to use low pass filter to avoid integration drift [12], however, this results in magnitude and phase error of the estimated flux. Implementing a pure integrator avoids the bandwidth limitation associated with low pass filter, especially at low frequencies [13].

The modified block diagram of stator flux vector control scheme is represented in Fig. (1) and the motor torque is expressed as a cross product of the stator and rotor flux as in equation(11).

$$T_d = \frac{3}{2} P \frac{L_m}{\sigma L_s L_r} \left(\psi_{r\alpha} \cdot \psi_{s\beta} - \psi_{r\beta} \cdot \psi_{s\alpha} \right) \quad (11)$$

and the motion equation is as follow:

$$\frac{T_e - T_L}{J} = P \frac{d\omega_r}{dt} + B * \omega_r \quad (12)$$

Where: P is the number of pair poles, J is the combined rotor and load inertia coefficient, β is the combined rotor and load friction coefficient. In similar to rotor field orientation the stator flux components can be written in synchronous reference frame as follow:

$$\psi^{*e}_{ds} = \frac{Ls}{Lm} * (1 + \sigma T_r * P) \lambda^*_r \quad (13)$$

$$\psi^{*e}_{qs} = \frac{2\sigma LsLr}{3PLm} * \frac{T_e^*}{\psi r^*} \quad (14)$$

In equation (4) it is clear that a change in the control variables y_{ds} in synchronous reference frame is followed with a time constant T_r which is much lower than the rotor time constant T_r involved in traditional stator current control and this gives the facility to faster controller. From equation (5) it is noticed that with constant rotor flux command a change in y_{qs} is followed by a corresponding change in torque and this will give decoupling. In principle, the control method proposed here is based on driving the stator flux vector toward its reference vector by applying the appropriate voltage vector and a normal PWM method to obtain constant switching frequency and reduced torque pulsations. The synchronous frame flux regulator requires d-q to a-b-c additional transformation and the angle of transformation can be calculated as follows, As a simple solution to delete d-q to a-b-c additional transformation and then the control algorithm will be nearly similar to standard DTC which has the advantage of no reference frame transformation. The motor slip angle will be calculated through torque comparator and PI controller as shown in Fig. (1). The angle of the stator flux can be obtained easily in stator reference frame using the rotor position through a position sensor or a sensor less solution in addition to the slip angle which has been calculated.

4. SIMULATION RESULTS

The developed control system has been implemented in a computer simulation program, modeling the two subsystem induction motor and control algorithm. The controller simulation uses the parameters of an experimental laboratory prototype. These parameters are listed in the Appendix. The graphs shown in Fig.(5) depict the response of the system with a torque command of 4 N.m. The transient and steady state flux vector in Fig.(5-a) shows nearly a circular path indicating a good flux regulation. The electromagnetic torque shown in Fig.(5-b) is close to the commanded value, while the time taken for the torque reach its commanded value is about 0.02 Sec., ensuring good dynamic torque response. Fig.(5-c) shows the stator currents in phase a, b and c which are nearly sinusoidal. Fig.(5-d) shows the waveforms of stator currents in d-q axis, it is noticed that the phase shift between them equal 90^0.

Figure(6) shows the response of the system for a step change in torque from 3 N.m. to 7 N.m. keeping the flux command constant. Fig.(6-a) shows the steady state stator flux, which demonstrates an excellent dynamic flux control under changed command torque. Fig.(6-b) shows the developed torque which is enclosed to a commanded value of 3 N.m. region or 7 N.m. region. The three phase stator currents are shown in Fig.(6-c). It is clear that, these stator currents are changed at the instant of changing the command torque and swiftly retrieve their steady state values.

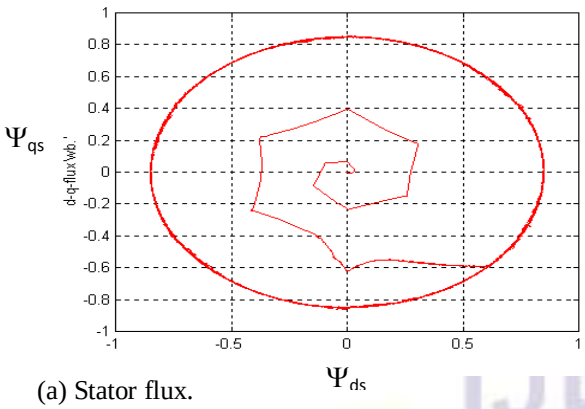

(a) Stator flux.

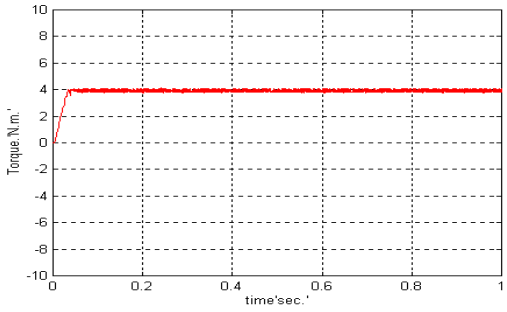

(b) Electromagnetic torque.

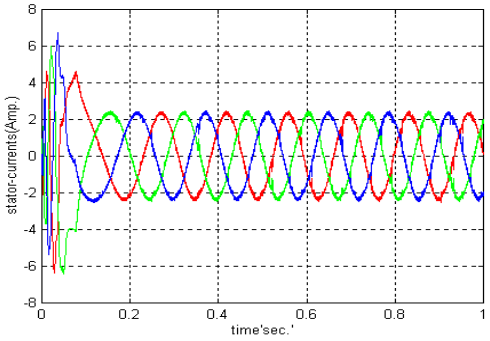

(c) Stator currents.

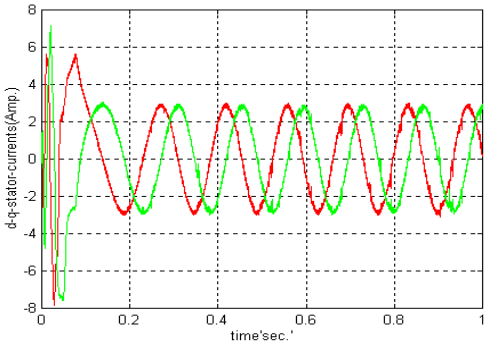

(d) d-q axis stator current.

Fig. (5) System response at load torque 4 N.m. and motor speed 1500 rpm.

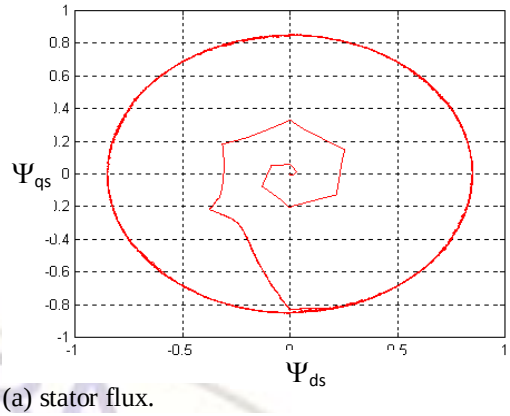

(a) stator flux.

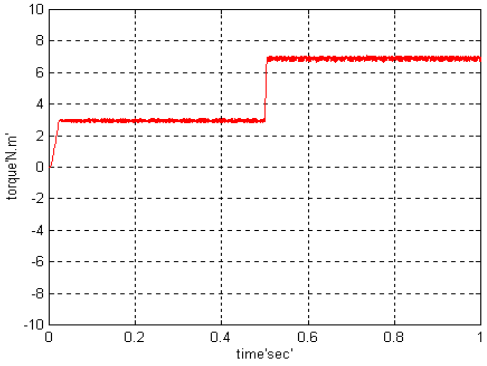

(b) Electromagnetic torque.

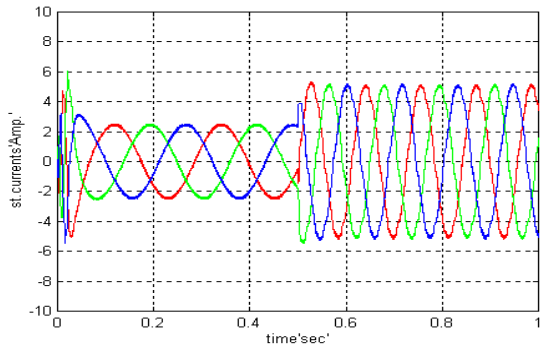

(c) Stator currents.

Fig. (6) System response for step change in load torque.

Figure(7) shows simulation results in which a step response of the system is studied at a step change of command torque from 3 N.m. to its 7 N.m. at 0.4 Sec., then, at 0.8 Sec. the command torque is decreased to its initial value (3 N.m.). Behavior of developed torque shows clearly that the response of the torque is as quickly as possible as shown in Fig.(7-b). As can be seen from Fig.(7-c), it is clear that, the stator currents in phases a, b, and c are changing according to the variation of the command torque. The values of currents in the region, where the torque is increased to 7 N.m, is increased to 3.5 Amp.(r.m.s.).

5. EXPERIMENTAL IMPLEMENTATION

Several dynamic tests were performed to investigate the validity of the proposed control method. The experimental set-up used for the practical investigation is shown in Fig.(8). The induction motor under test is coupled to a self-excited DC generator. The motor is energized from an inverter bridge, which consists of six IGBTs in conjunction with stepper circuits. The DC-link is provided from three-phase bridge rectifier. An incremental encoder is coupled to the motor shaft to measure the motor speed. Actual stator currents are measured using current sensors. The stator voltages are sensed using voltage transducers. This system is fully controlled by a DSP controller board which is installed on a PC computer.

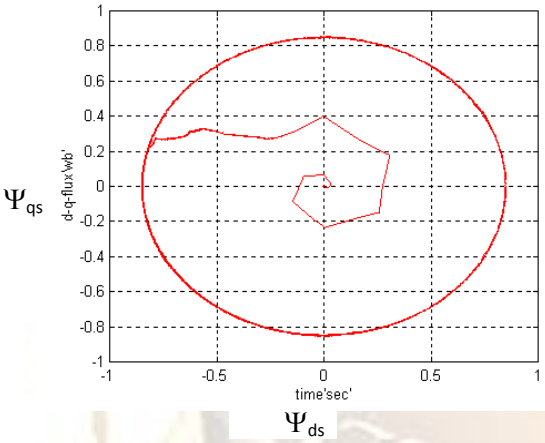

(a) stator flux.

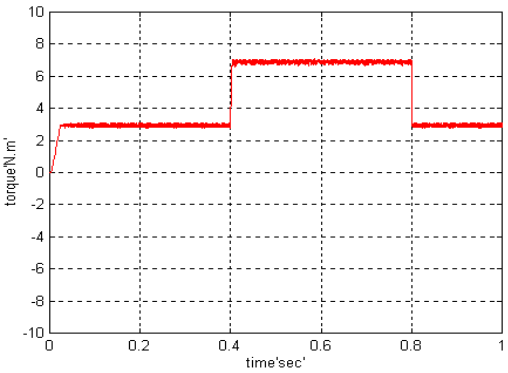

(b) Electromagnetic torque.

Fig. (7) System response for step change in load torque.

A series of experimental results was carried out to verify the validity of the proposed control scheme for the drive system. The results were obtained at different operating points. The results were obtained at different operating points. First, the drive system response was obtained at heavy load and a speed below the base speed. Figure (9) shows the motor speed response at 1200 rpm. The motor started with almost no overshoot and follows its command with nearly zero steady state error. The motor phase currents are also shown in Fig. (9).

The response of the control system due to a step change in speed command is shown in Fig. (10). The speed command is changed from 120 rad/s to 100 rad/s. It can be seen from Fig. (10) that the motor speed is decelerated smoothly to follow its reference value. Figure (11), show the motor response for step up in speed command, which change from 100 rad/s to 150 rad/s.

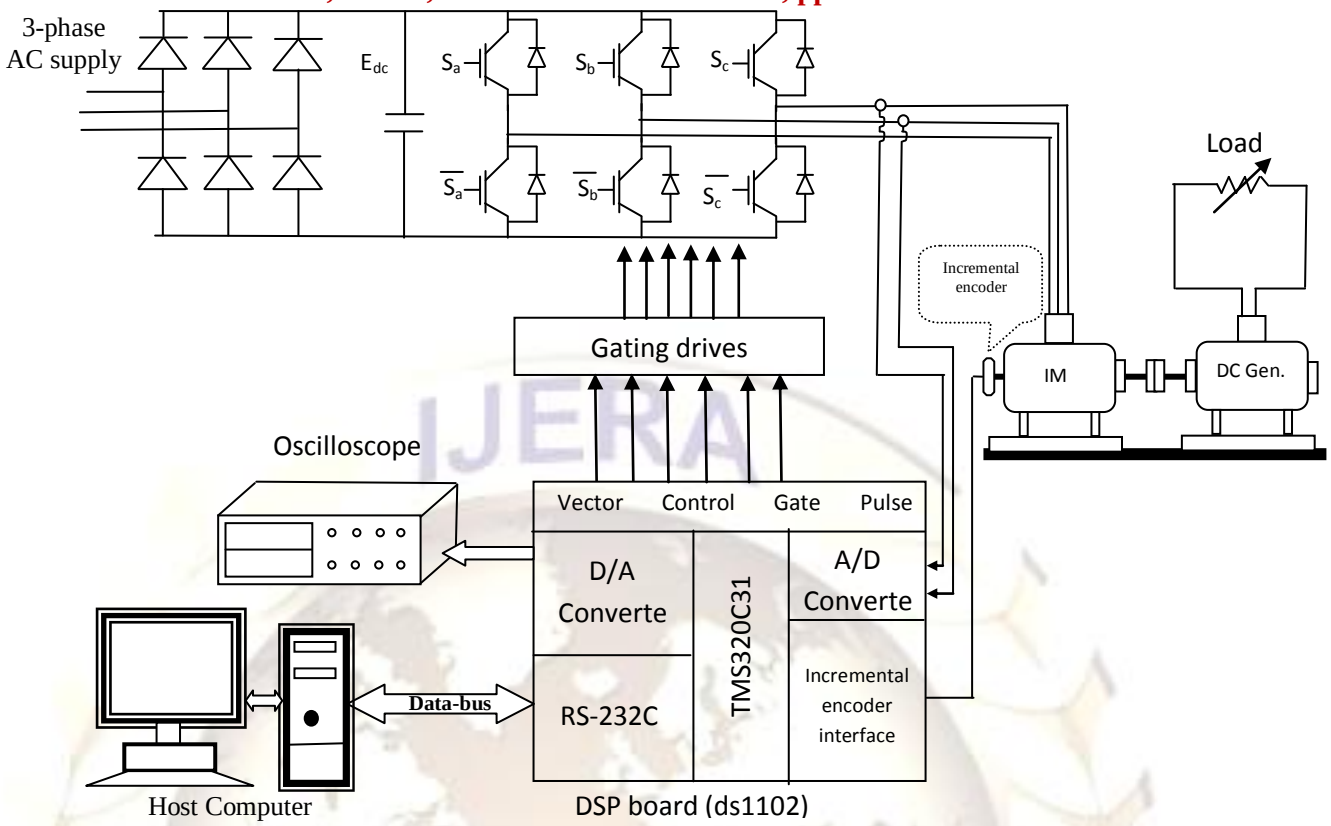

Fig. (8) Experimental set-up for DSP-based control of IM drive

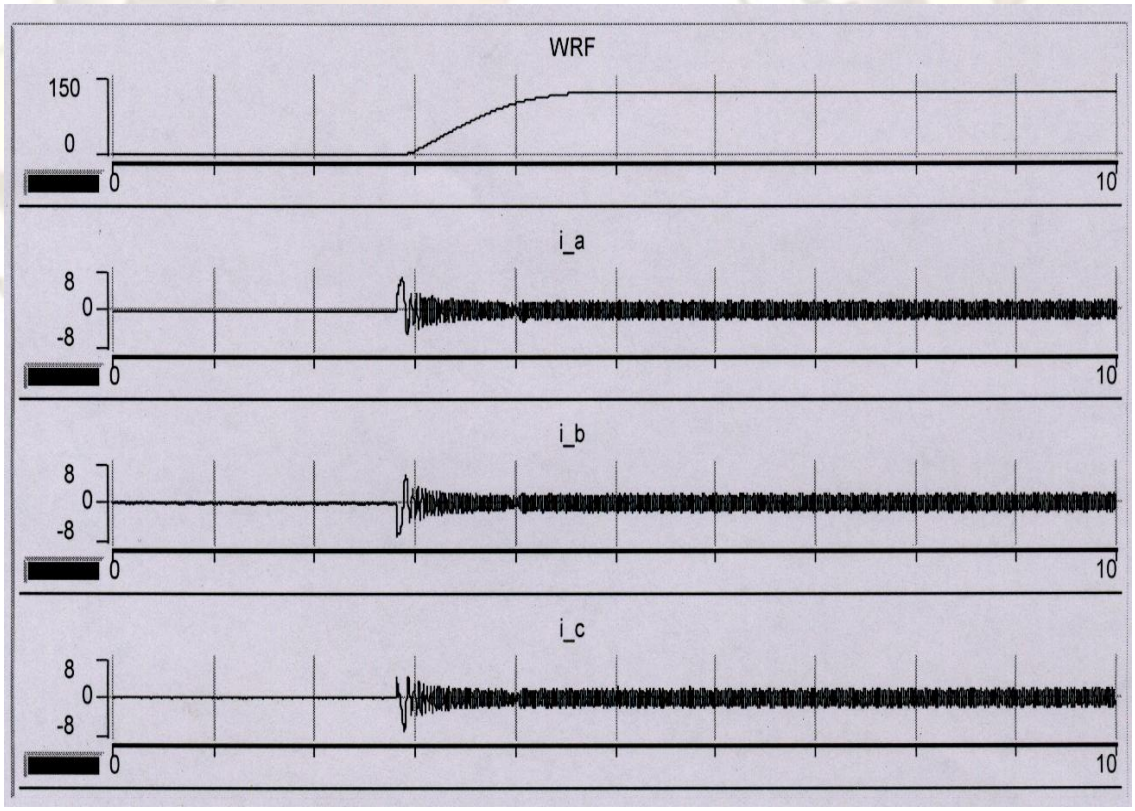

Fig. (9) Drive response for reference speed of 1200 rpm (x-axis Time (ms))

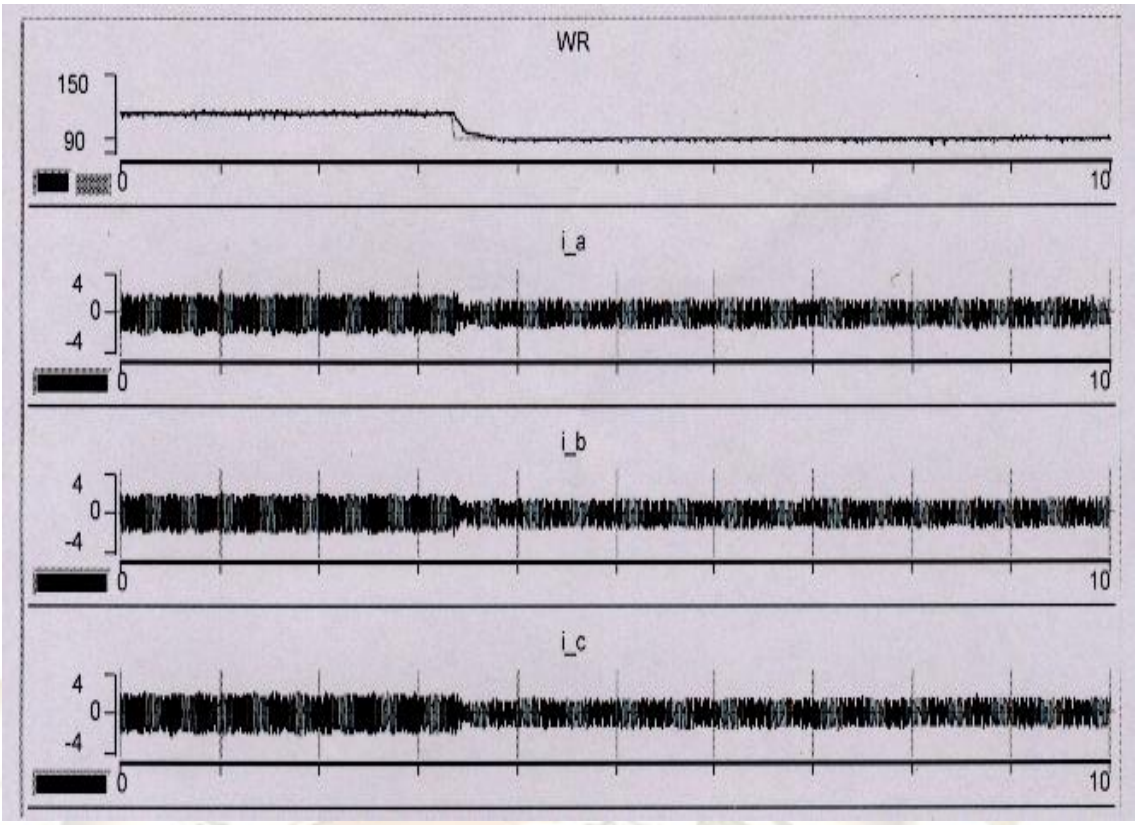

Fig. (10) System performance for step down in speed command (x-axis Time (ms))

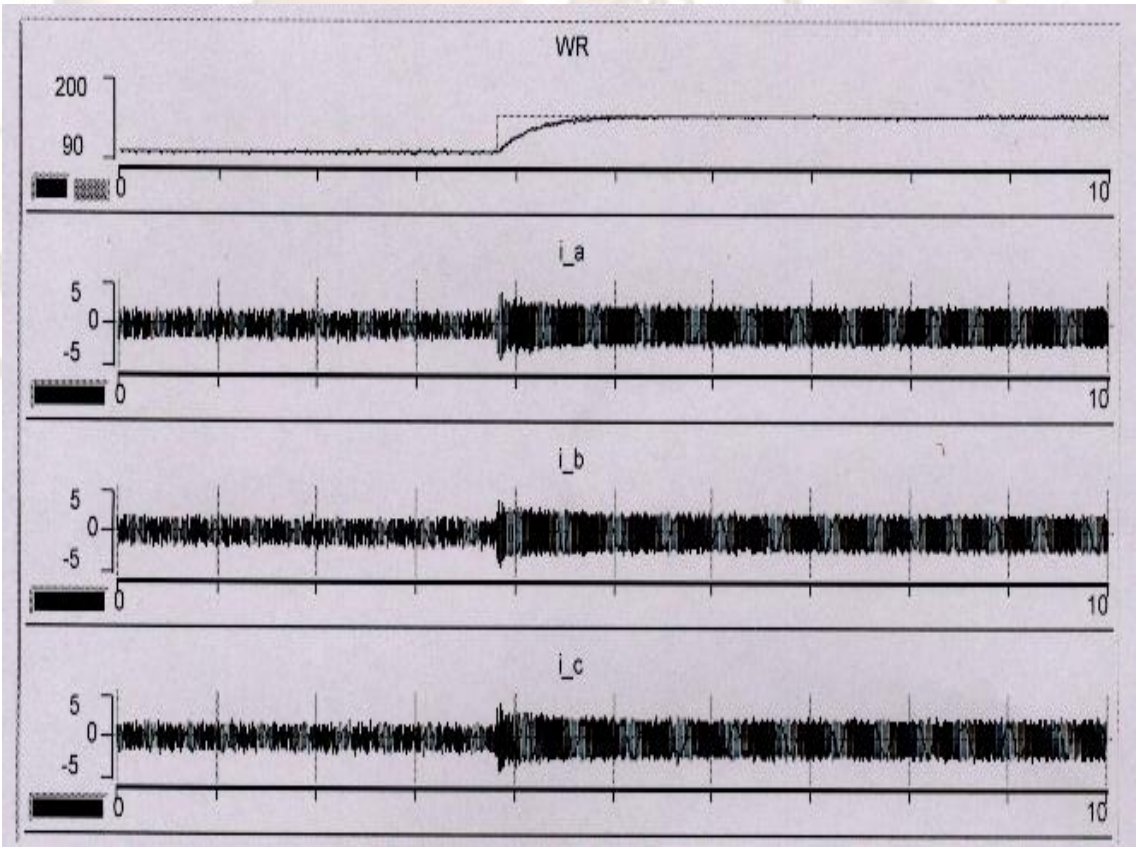

Fig. (11) System performance for step up in speed command (x-axis Time (ms))

6. CONCLUSIONS

In this paper, the basic concept of DTC is implemented using a DSP control system by modifying the classical method. The advantage of the proposed method lies in achieving constant switching frequency and solving the starting problem without a dither signal. A further improvement of this work can be achieved by using stator flux estimation and reduced torque pulsation techniques. The existence of non linear torque and flux hysteresis controllers result in noticeable torque pulsations and variable switching frequency. Thus, the proposed control method can give transient performance like DTC and reduced torque pulsations at steady state. An inverter switching pattern that can achieve DTC method for induction motors in which the analytical derivation is based on the prediction of the voltage vector direction which is required to compensate electromagnetic torque and stator flux errors. In general, an optimistic experimental results and an improved performance over other existing schemes is obtained.

REFERENCES

[1] J. Holtz and J. Quan " Sensorless Vector Control of Induction Motor at Very Low Speed Using a Non Linear Inverter Model and Parameter Identification," IEEE Transaction Industry Applications Society Annual Meeting, Chicago, Sept. 30- Oct. 4, 2001.

[2] M. Depenbrock, " Direct Self Control (DSC) of Inverter-fed Induction Motors, " IEEE Transaction Power Electronics, Vol. 3, No. 4, pp. 420-429, October1988.

[3] I. Takahashi and T. Noguchi " A new Quick Response and High Efficiency Control Strategy of An Induction Motor, " IEEE Transaction Industry Applications, Vol. IA-22, No.5, PP. 820-827, .Sept./Oct. 1986.

[4] E. Flach, R. Hoffmann, P. Mutschler " Direct Mean Torque Control of Induction Motor, " in Conf. Rec. of the European Conference on Power Electronics and Applications, pp. 3672-3676, 1997.

[5] E. E. El-Kholy , S. A. Mahmoud, R. Kennel, A. El-Refaei, and F. El-Kady, "Torque Ripple Minimization for Induction Motor Drives With Direct Torque Control" Electrical Power Components and Systems Journal, Vol. 33, No. 8, pp. 845-859, August 2005.

[6] E. E. El-Kholy , S. A. Mahmoud, R. Kennel, A. El-Refaei, and F. El-Kady, "Analysis and Implementation of a New Space-Vector Current Regulation for Induction Motor Drives" Electrical Power Components and Systems Journal, Vol. 34, No. 3, pp. 303-319, March 2006.

[7] A. Linder: " A Rapid-Prototyping System Based on Standard PCs with RTAI as Real-Time Operating System, " Third Real-Time Linux Workshop, Milan, Italy, November 26 -29, 2001

[8] R. Kennel, A. El-refaei, F. Elkady, E. Elkholy and S. A. Mahmoud "Improved direct torque control for induction motor drives with rapid prototyping system" IEEE, IECON, 2003 U.S.A.

[9] R. Kennel, A. El-refaei, F. Elkady, E. Elkholy and S. A. Mahmoud " Torque Ripple Minimization for Induction Motor Drives with Direct Torque Control (DTC), "The Fifth International Conference on Power Electronics and Drive Systems PEDS 2003, Singapore, November 17 – 20, 2003.

[10] J. Chen. Yongdong " Virtual Vectors Based Predictive Control of Torque and Flux of Induction Motor and Speed Sensorless Drives, " IEEE, IECON 1999.

[11] Y. Xue, X. Xu, T. G. Habetler and D. M. Divan " A Stator Flux-Oriented Voltage Source Variable-Speed Drive Based on dc Link Measurement," IEEE Transaction Industry applications, Vol. 27, No. 5, pp. 962-969, September/October 1991.

[12] T. G. Habetler, F. Profumo, G. Griva " Stator Resistance Tuning In A stator Flux Field Oriented Drive Using An Instantaneous Hybrid Flux Estimator, " The European Power Electronics Association, Brighton, No. 13, pp. 292-299, September, 1993.

[13] N. R. Idris, A. Halim, N. A. Azly, " Direct Torque Control of Induction Machines With Constant Switching Frequency and Improved Stator Flux Estimation," 27th Annual Conference of the IEEE Ind. Elect. Society, pp. 1285-1291.

[14] L. Jansen, D. Lorenz "Observer Based Direct Field Orientation Analysis and Comparison of Alternative Methods," IEEE Transaction Industry applications, Vol. 30, No. 4, pp. 945-953, July /August 1994.

[15] B. Kenny, D. Lorenz " Deadbeat Direct Torque Control Of Induction Machines Using Self Sensing at low and zero speed, " Ph. D thesis Wosconsin, Madison, U. S. A., 2001.

[16] J. Holtz, J. Quan " Sensorless Vector Control of Induction Motors at Very Low Speed, " Ph. D thesis, Wuppertal university, 2002.

[17] A. B. Plunkett, J. D. D'atre, and T. A. Lipo," Synchronous Control of Static AC

Induction Motor Drive, " IEEE Trans. On Industry Applications, Vol. IA-15, No.4, pp. 430-437, July/August 1979.

[18] D. Casadei, G. Serra, A. Tani, L. Zarri " Performance Analysis of a Speed Sensorless Induction Motor drive Based on a Constant Switching Frequency DTC Scheme, " IEEE, IECON, 2000.

[19] Habetler "Direct Torque control of an Induction Machines Using Space Vector Modulation," IEEE Transaction Industry Applications, Vol. 28, No. 5, pp. 11045-1053, September/October 1992.

[20] J. Monteiro, G. Marques, and J. Palma "A Simplified Stator Flux Vector Control Method in d-q Co-ordinates For Induction Machines," ISIE 2000.

I. Appendix

The induction motor is a squirrel cage and has the following data:

Rated power	: 1.1 KW
Rated line voltage	: 380 volt.
No. of pole pair	: 2.0
Stator resistance	: 4. 4826 ohm.
Rotor resistance	: 3. 6840 ohm.
Stator leakage inductance	: 0.0221 Henry.
Rotor leakage inductance	: 0.0221 Henry.
Mutual inductance	: 0.4114 Henry.
Supply frequency	: 50.0
Rated load torque	: 11.0 N. m.